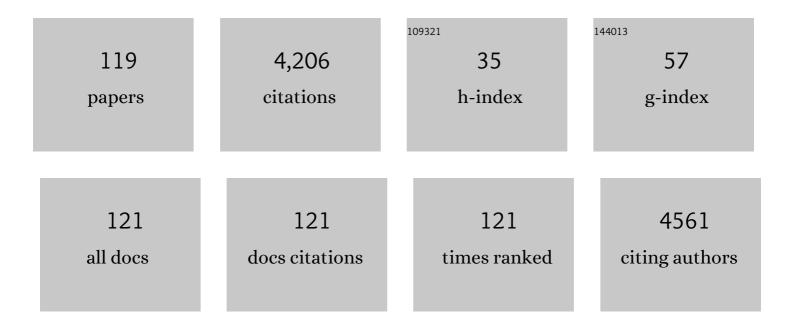
Yanlei Wang

List of Publications by Year in descending order

Source: https://exaly.com/author-pdf/1927228/publications.pdf Version: 2024-02-01



YANLEI MANC

#	Article	lF	CITATIONS
1	Super-tough MXene-functionalized graphene sheets. Nature Communications, 2020, 11, 2077.	12.8	289
2	Initiating Hexagonal MoO ₃ for Superb‣table and Fast NH ₄ ⁺ Storage Based on Hydrogen Bond Chemistry. Advanced Materials, 2020, 32, e1907802.	21.0	186
3	Multifunctional Pristine Chemically Modified Graphene Films as Strong as Stainless Steel. Advanced Materials, 2015, 27, 6708-6713.	21.0	157
4	Measuring Interlayer Shear Stress in Bilayer Graphene. Physical Review Letters, 2017, 119, 036101.	7.8	155
5	Strong sequentially bridged MXene sheets. Proceedings of the National Academy of Sciences of the United States of America, 2020, 117, 27154-27161.	7.1	148
6	Ultrastrong Graphene Films via Long-Chain π-Bridging. Matter, 2019, 1, 389-401.	10.0	108
7	Synergistic Regulation of Polysulfides Conversion and Deposition by MOFâ€Derived Hierarchically Ordered Carbonaceous Composite for Highâ€Energy Lithium–Sulfur Batteries. Advanced Functional Materials, 2019, 29, 1900875.	14.9	104
8	Design and Fabrication of Silk Templated Electronic Yarns and Applications in Multifunctional Textiles. Matter, 2019, 1, 1411-1425.	10.0	98
9	Recent progress in theoretical and computational studies on the utilization of lignocellulosic materials. Green Chemistry, 2019, 21, 9-35.	9.0	96
10	Behavior of Circular Fiber-Reinforced Polymer–Steel-Confined Concrete Columns Subjected to Reversed Cyclic Loads: Experimental Studies and Finite-Element Analysis. Journal of Structural Engineering, 2019, 145, .	3.4	96
11	Properties and mechanisms of self-sensing carbon nanofibers/epoxy composites for structural health monitoring. Composite Structures, 2018, 200, 669-678.	5.8	84
12	Monotonic axial compressive behaviour and confinement mechanism of square CFRP-steel tube confined concrete. Engineering Structures, 2020, 217, 110802.	5.3	75
13	Ultratough graphene–black phosphorus films. Proceedings of the National Academy of Sciences of the United States of America, 2020, 117, 8727-8735.	7.1	74
14	Axial compressive behavior and confinement mechanism of circular FRP-steel tubed concrete stub columns. Composite Structures, 2021, 256, 113082.	5.8	72
15	Highly Efficient Photothermal Conversion and Water Transport during Solar Evaporation Enabled by Amorphous Hollow Multishelled Nanocomposites. Advanced Materials, 2022, 34, e2107400.	21.0	68
16	Spider-Web-Inspired Nanocomposite-Modified Separator: Structural and Chemical Cooperativity Inhibiting the Shuttle Effect in Li–S Batteries. ACS Nano, 2019, 13, 1563-1573.	14.6	65
17	Behavior of circular ice-filled self-luminous FRP tubular stub columns under axial compression. Construction and Building Materials, 2020, 232, 117287.	7.2	65
18	High CO2 absorption capacity of metal-based ionic liquids: A molecular dynamics study. Green Energy and Environment, 2021, 6, 253-260.	8.7	60

#	Article	IF	CITATIONS
19	Strain and damage self-sensing of basalt fiber reinforced polymer laminates fabricated with carbon nanofibers/epoxy composites under tension. Composites Part A: Applied Science and Manufacturing, 2018, 113, 40-52.	7.6	55
20	Hierarchical Grapheneâ€Based Films with Dynamic Selfâ€6tiffening for Biomimetic Artificial Muscle. Advanced Functional Materials, 2016, 26, 7003-7010.	14.9	53
21	Intercalated water layers promote thermal dissipation at bio–nano interfaces. Nature Communications, 2016, 7, 12854.	12.8	52
22	Primary Nucleation-Dominated Chemical Vapor Deposition Growth for Uniform Graphene Monolayers on Dielectric Substrate. Journal of the American Chemical Society, 2019, 141, 11004-11008.	13.7	52
23	Sequential drug release via chemical diffusion and physical barriers enabled by hollow multishelled structures. Nature Communications, 2020, 11, 4450.	12.8	52
24	Interfacial Engineering Promoting Electrosynthesis of Ammonia over Mo/Phosphotungstic Acid with High Performance. Advanced Functional Materials, 2021, 31, 2009151.	14.9	47
25	Strain monitoring of concrete components using embedded carbon nanofibers/epoxy sensors. Construction and Building Materials, 2018, 186, 367-378.	7.2	44
26	Molecular Insights into the Regulatable Interfacial Property and Flow Behavior of Confined Ionic Liquids in Graphene Nanochannels. Small, 2019, 15, e1804508.	10.0	44
27	Characterizing phonon thermal conduction in polycrystalline graphene. Journal of Materials Research, 2014, 29, 362-372.	2.6	42
28	Insights into Ionic Liquids: From Z-Bonds to Quasi-Liquids. Jacs Au, 2022, 2, 543-561.	7.9	42
29	A new era of precise liquid regulation: Quasi-liquid. Green Energy and Environment, 2017, 2, 329-330.	8.7	40
30	Nature-Inspired 2D-Mosaic 3D-Gradient Mesoporous Framework: Bimetal Oxide Dual-Composite Strategy toward Ultrastable and High-Capacity Lithium Storage. ACS Nano, 2018, 12, 2035-2047.	14.6	40
31	The confined [Bmim][BF ₄] ionic liquid flow through graphene oxide nanochannels: a molecular dynamics study. Physical Chemistry Chemical Physics, 2018, 20, 17773-17780.	2.8	40
32	Preparation of MWCNTs-Graphene-Cellulose Fiber with Ionic Liquids. ACS Sustainable Chemistry and Engineering, 2019, 7, 20013-20021.	6.7	40
33	Interphase Induced Dynamic Selfâ€ S tiffening in Grapheneâ€Based Polydimethylsiloxane Nanocomposites. Small, 2016, 12, 3723-3731.	10.0	39
34	Understanding the Antifouling Mechanism of Zwitterionic Monomer-Grafted Polyvinylidene Difluoride Membranes: A Comparative Experimental and Molecular Dynamics Simulation Study. ACS Applied Materials & Interfaces, 2019, 11, 14408-14417.	8.0	39
35	Unraveling the Synergistic Coupling Mechanism of Li ⁺ Transport in an "lonogelâ€in eramic― Hybrid Solid Electrolyte for Rechargeable Lithium Metal Battery. Advanced Functional Materials, 2022, 32, 2108706.	14.9	38
36	Suppressing surface passivation of bimetallic phosphide by sulfur for long-life alkaline aqueous zinc batteries. Energy Storage Materials, 2020, 33, 230-238.	18.0	36

#	Article	IF	CITATIONS
37	Hygrothermal ageing behavior and mechanism of carbon nanofibers modified flax fiber-reinforced epoxy laminates. Composites Part A: Applied Science and Manufacturing, 2021, 140, 106142.	7.6	36
38	Confined, Oriented, and Electrically Anisotropic Graphene Wrinkles on Bacteria. ACS Nano, 2016, 10, 8403-8412.	14.6	35
39	Interlayer Coupling Behaviors of Boron Doped Multilayer Graphene. Journal of Physical Chemistry C, 2017, 121, 26034-26043.	3.1	33
40	Behavior of innovative circular ice filled steel tubular stub columns under axial compression. Construction and Building Materials, 2018, 171, 680-689.	7.2	32
41	Molecular mechanism of anion size regulating the nanostructure and charging process at ionic liquid–electrode interfaces. Journal of Materials Chemistry A, 2020, 8, 19908-19916.	10.3	31
42	The Ionic Liquid–H ₂ O Interface: A New Platform for the Synthesis of Highly Crystalline and Molecular Sieving Covalent Organic Framework Membranes. ACS Applied Materials & Interfaces, 2021, 13, 36507-36516.	8.0	31
43	Reconstructing Vanadium Oxide with Anisotropic Pathways for a Durable and Fast Aqueous K-Ion Battery. ACS Nano, 2021, 15, 17717-17728.	14.6	30
44	Structure Evolution of Graphene Oxide during Thermally Driven Phase Transformation: Is the Oxygen Content Really Preserved?. PLoS ONE, 2014, 9, e111908.	2.5	29
45	Mechanical responses of boron-doped monolayer graphene. Carbon, 2019, 147, 594-601.	10.3	28
46	Tailoring Multiple Sites of Metal–Organic Frameworks for Highly Efficient and Reversible Ammonia Adsorption. ACS Applied Materials & Interfaces, 2021, 13, 56025-56034.	8.0	28
47	Water Intercalation for Seamless, Electrically Insulating, and Thermally Transparent Interfaces. ACS Applied Materials & Interfaces, 2016, 8, 1970-1976.	8.0	27
48	Lower Limit of Interfacial Thermal Resistance across the Interface between an Imidazolium Ionic Liquid and Solid Surface. Journal of Physical Chemistry C, 2018, 122, 22194-22200.	3.1	27
49	Ionophobic nanopores enhancing the capacitance and charging dynamics in supercapacitors with ionic liquids. Journal of Materials Chemistry A, 2021, 9, 15985-15992.	10.3	27
50	Hygrothermal aging behavior and aging mechanism of carbon nanofibers/epoxy composites. Construction and Building Materials, 2021, 294, 123538.	7.2	27
51	Continuous Energy Harvesting from Ubiquitous Humidity Gradients using Liquidâ€Infused Nanofluidics. Advanced Materials, 2022, 34, e2106410.	21.0	27
52	The critical power to maintain thermally stable molecular junctions. Nature Communications, 2014, 5, 4297.	12.8	26
53	Structure and interaction properties of MBIL [Bmim][FeCl4] and methanol: A combined FTIR and simulation study. Journal of Molecular Liquids, 2020, 309, 113061.	4.9	26
54	Unleashing ultra-fast sodium ion storage mechanisms in interface-engineered monolayer MoS ₂ /C interoverlapped superstructure with robust charge transfer networks. Journal of Materials Chemistry A, 2020, 8, 15002-15011.	10.3	26

#	Article	IF	CITATIONS
55	An effective interface-regulating mechanism enabled by non-sacrificial additives for high-voltage nickel-rich cathode. Journal of Power Sources, 2020, 453, 227852.	7.8	26
56	"Mix-Then-On-Demand-Complex― <i>In Situ</i> Cascade Anionization and Complexation of Graphene Oxide for High-Performance Nanofiltration Membranes. ACS Nano, 2021, 15, 4440-4449.	14.6	26
57	Ultralow Thermal Resistance across the Solid–Ionic Liquid Interface Caused by the Charge-Induced Ordered Ionic Layer. Industrial & Engineering Chemistry Research, 2019, 58, 20109-20115.	3.7	25
58	Characterizing the impact of surfactant structure on interfacial tension: a molecular dynamics study. Journal of Molecular Modeling, 2017, 23, 112.	1.8	24
59	Theoretical Elucidation of β-O-4 Bond Cleavage of Lignin Model Compound Promoted by Sulfonic Acid-Functionalized Ionic Liquid. Frontiers in Chemistry, 2019, 7, 78.	3.6	24
60	Interfacial behaviors of betaine and binary betaine/carboxylic acid mixtures in molecular dynamics simulation. Journal of Molecular Liquids, 2017, 240, 412-419.	4.9	23
61	Effect of specimen thicknesses on water absorption and flexural strength of CFRP laminates subjected to water or alkaline solution immersion. Construction and Building Materials, 2019, 208, 314-325.	7.2	22
62	Height-driven structure and thermodynamic properties of confined ionic liquids inside carbon nanochannels from molecular dynamics study. Physical Chemistry Chemical Physics, 2019, 21, 12767-12776.	2.8	22
63	Mesoscale structures and mechanisms in ionic liquids. Particuology, 2020, 48, 55-64.	3.6	22
64	In situ growth of nano-antioxidants on cellular vesicles for efficient reactive oxygen species elimination in acute inflammatory diseases. Nano Today, 2021, 40, 101282.	11.9	22
65	Behavior and design-oriented model for elliptical FRP-confined concrete under axial compression. Engineering Structures, 2021, 249, 113387.	5.3	22
66	Out-of-Plane Deformations Determined Mechanics of Vanadium Disulfide (VS ₂) Sheets. ACS Applied Materials & Interfaces, 2021, 13, 3040-3050.	8.0	21
67	Mechanical Behavior of BFRP-Steel Composite Plate under Axial Tension. Polymers, 2014, 6, 1862-1876.	4.5	20
68	Regulated interfacial stability by coordinating ionic liquids with fluorinated solvent for high voltage and safety batteries. Journal of Power Sources, 2021, 491, 229603.	7.8	20
69	Superflexible C ₆₈ -graphyne as a promising anode material for lithium-ion batteries. Journal of Materials Chemistry A, 2019, 7, 17357-17365.	10.3	19
70	Comparison of monotonic axial compressive behavior of rectangular concrete confined by FRP with different rupture strains. Construction and Building Materials, 2021, 299, 124241.	7.2	19
71	Bond durability and degradation mechanism of GFRP bars in seawater sea-sand concrete under the coupling effect of seawater immersion and sustained load. Construction and Building Materials, 2021, 307, 124878.	7.2	19
72	Atomistic dynamics of sulfur-deficient high-symmetry grain boundaries in molybdenum disulfide. Nanoscale, 2017, 9, 10312-10320.	5.6	18

#	Article	IF	CITATIONS
73	Axial compressive behavior of square ice filled steel tubular stub columns. Construction and Building Materials, 2018, 188, 198-209.	7.2	18
74	Intensified Energy Storage in High-Voltage Nanohybrid Supercapacitors <i>via</i> the Efficient Coupling between TiNb ₂ O ₇ /Holey-rGO Nanoarchitectures and Ionic Liquid-Based Electrolytes. ACS Applied Materials & Interfaces, 2021, 13, 21349-21361.	8.0	18
75	Mechanical responses of the bio-nano interface: A molecular dynamics study of graphene-coated lipid membrane. Theoretical and Applied Mechanics Letters, 2015, 5, 231-235.	2.8	17
76	Thermal transport in oxidized polycrystalline graphene. Carbon, 2016, 108, 318-326.	10.3	17
77	Solid–Liquid Electrolyte as a Nanoion Modulator for Dendrite-Free Lithium Anodes. ACS Applied Materials & Interfaces, 2018, 10, 20412-20421.	8.0	17
78	In Situ Strain and Damage Monitoring of GFRP Laminates Incorporating Carbon Nanofibers under Tension. Polymers, 2018, 10, 777.	4.5	17
79	Tailoring sensing properties of smart cementitious composites based on excluded volume theory and electrostatic self-assembly. Construction and Building Materials, 2020, 256, 119452.	7.2	17
80	Assessment of Selfâ€Assembled Monolayers as Highâ€Performance Thermal Interface Materials. Advanced Materials Interfaces, 2017, 4, 1700355.	3.7	16
81	Data-Driven Discovery and Understanding of Ultrahigh-Modulus Crystals. Chemistry of Materials, 2021, 33, 1276-1284.	6.7	16
82	Understanding Structural and Transport Properties of Dissolved Li ₂ S ₈ in Ionic Liquid Electrolytes through Molecular Dynamics Simulations. ChemPhysChem, 2021, 22, 419-429.	2.1	16
83	Topological engineering of two-dimensional ionic liquid islands for high structural stability and CO ₂ adsorption selectivity. Chemical Science, 2021, 12, 15503-15510.	7.4	16
84	Neuron-Mimic Smart Electrode: A Two-Dimensional Multiscale Synergistic Strategy for Densely Packed and High-Rate Lithium Storage. ACS Nano, 2019, 13, 9148-9160.	14.6	15
85	A space-confined strategy toward large-area two-dimensional crystals of ionic liquid. Physical Chemistry Chemical Physics, 2020, 22, 1820-1825.	2.8	15
86	Abnormal Enhanced Free Ions of Ionic Liquids Confined in Carbon Nanochannels. Journal of Physical Chemistry Letters, 2021, 12, 6078-6084.	4.6	15
87	Theoretical Insights Into the Depolymerization Mechanism of Lignin to Methyl p-hydroxycinnamate by [Bmim][FeCl4] Ionic Liquid. Frontiers in Chemistry, 2019, 7, 446.	3.6	14
88	Effect of Clusters on [Li] Solvation and Transport in Mixed Organic Compound/Ionic Liquid Electrolytes under External Electric Fields. Industrial & Engineering Chemistry Research, 2020, 59, 11308-11316.	3.7	14
89	Molecular Insights into the Abnormal Wetting Behavior of Ionic Liquids Induced by the Solidified Ionic Layer. Industrial & Engineering Chemistry Research, 2020, 59, 8028-8036.	3.7	14
90	Ionic liquids screening for lignin dissolution: COSMO-RS simulations and experimental characterization. Journal of Molecular Liquids, 2022, 348, 118007.	4.9	14

#	Article	IF	CITATIONS
91	Strain and damage self-sensing properties of carbon nanofibers/carbon fiber–reinforced polymer laminates. Advances in Mechanical Engineering, 2017, 9, 168781401668864.	1.6	13
92	Entropy driving highly selective CO2 separation in nanoconfined ionic liquids. Chemical Engineering Journal, 2022, 440, 135918.	12.7	13
93	A new thickness-based accelerated aging test methodology for resin materials: Theory and preliminary experimental study. Construction and Building Materials, 2018, 186, 986-995.	7.2	12
94	First-principles study on screening doped TiO2(B) as an anode material with high conductivity and low lithium transport resistance for lithium-ion batteries. Physical Chemistry Chemical Physics, 2019, 21, 17985-17992.	2.8	12
95	Behavior and Modeling of Circular Large Rupture Strain FRP-Confined Ice under Axial Compression. Journal of Composites for Construction, 2021, 25, .	3.2	12
96	Molecular thermodynamic understanding of transport behavior of <scp>CO₂</scp> at the ionic liquidsâ€electrode interface. AICHE Journal, 2021, 67, e17060.	3.6	12
97	Circadian humidity fluctuation induced capillary flow for sustainable mobile energy. Nature Communications, 2022, 13, 1291.	12.8	12
98	Tensile strain and damage self-sensing of flax FRP laminates using carbon nanofiber conductive network coupled with acoustic emission. Composite Structures, 2022, 290, 115549.	5.8	11
99	Thermodynamical Origin of Nonmonotonic Inserting Behavior of Imidazole Ionic Liquids into the Lipid Bilayer. Journal of Physical Chemistry Letters, 2021, 12, 9926-9932.	4.6	9
100	Axial compressive behavior and modeling of fiber-reinforced polymer-concrete-steel double-skin tubular stub columns with a rectangular outer tube and an elliptical inner tube. Engineering Structures, 2022, 260, 114222.	5.3	9
101	Mechanistic transition of heat conduction in two-dimensional solids: A study of silica bilayers. Physical Review B, 2015, 92, .	3.2	8
102	Ionic liquid decoration for the hole transport improvement of PEDOT. Materials Advances, 2021, 2, 2009-2020.	5.4	8
103	Experimental study and piezoresistive mechanism of electrostatic self-assembly of carbon nanotubes–carbon black/epoxy nanocomposites for structural health monitoring. Journal of Materials Science, 2022, 57, 12416-12437.	3.7	7
104	Influence of Thickness on Water Absorption and Tensile Strength of BFRP Laminates in Water or Alkaline Solution and a Thickness-Dependent Accelerated Ageing Method for BFRP Laminates. Applied Sciences (Switzerland), 2020, 10, 3618.	2.5	6
105	Compressive Behavior of Circular Sawdust-Reinforced Ice-Filled Flax FRP Tubular Short Columns. Materials, 2020, 13, 957.	2.9	6
106	Understanding Electric Fieldâ€Dependent Structure Variation of Functional Ionic Liquids at the Electrode Interface. ChemElectroChem, 2021, 8, 1588-1595.	3.4	6
107	Experimental Investigation of a Self-Sensing Hybrid GFRP-Concrete Bridge Superstructure with Embedded FBG Sensors. International Journal of Distributed Sensor Networks, 2012, 8, 902613.	2.2	6
108	Machine Learning Screening of Efficient Ionic Liquids for Targeted Cleavage of the β–O–4 Bond of Lignin. Journal of Physical Chemistry B, 2022, 126, 3693-3704.	2.6	6

#	Article	IF	CITATIONS
109	A 3D molecular cantilever based on interfacial self-assembly and the cobra-like actuation of long-chain imidazolium ionic liquids. Nanoscale, 2019, 11, 7277-7286.	5.6	5
110	Performance and analysis of unidirectional GFRP actively confined high-strength concrete under monotonic and cyclic axial compression. Construction and Building Materials, 2021, 271, 121593.	7.2	5
111	Ionic Liquid-Based Extraction System for In-Depth Analysis of Membrane Protein Complexes. Analytical Chemistry, 2022, 94, 758-767.	6.5	5
112	Tracking the Microâ€Heterogeneity and Hydrogenâ€Bonding Interactions in Hydroxylâ€Functionalized Ionic Liquid Solutions: A Combined Experimental and Computational Study. ChemPhysChem, 2021, 22, 1891-1899.	2.1	4
113	Interfacial Proton Transfer for Hydrogen Evolution at the Sub-Nanometric Platinum/Electrolyte Interface. ACS Applied Materials & Interfaces, 2021, 13, 47252-47261.	8.0	4
114	A bioinspired interfacial design to toughen carbon nanotube fibers. Materials Chemistry Frontiers, 2021, 5, 5706-5717.	5.9	3
115	Balancing Anchoring and Diffusion for Screening of Metal Oxide Cathode Materials in Lithium–Sulfur Batteries. Journal of Physical Chemistry C, 2021, 125, 24318-24327.	3.1	3
116	Atomic structure and electrical property of ionic liquids at the MoS2 electrode with varying interlayer spacing. Journal of Molecular Modeling, 2021, 27, 41.	1.8	2
117	Smart heat isolator with hollow multishelled structures. Green Energy and Environment, 2023, 8, 1154-1160.	8.7	2
118	Probing Charge Injection-Induced Structural Transition in Ionic Liquids Confined at the MoS ₂ Surface. Industrial & Engineering Chemistry Research, 2021, 60, 7835-7843.	3.7	1
119	Compressive Behavior of Circular Sawdust-Reinforced Ice-Filled Large Rupture Strain Fiber-Reinforced Polymer Tubular Short Columns. Lecture Notes in Civil Engineering, 2022, , 1044-1054.	0.4	1